

An Integrated Device for the Solar-Driven Electrochemical Conversion of CO₂ to CO

Original

An Integrated Device for the Solar-Driven Electrochemical Conversion of CO₂ to CO / Sacco, Adriano; Speranza, Roberto; Savino, Umberto; Zeng, Juquin; Farkhondehfal, M. Amin; Lamberti, Andrea; Chiodoni, Angelica; Pirri, Candido F.. - In: ACS SUSTAINABLE CHEMISTRY & ENGINEERING. - ISSN 2168-0485. - ELETTRONICO. - 8:20(2020), pp. 7563-7568. [10.1021/acssuschemeng.0c02088]

Availability:

This version is available at: 11583/2837210 since: 2020-06-25T19:56:23Z

Publisher:

AMER CHEMICAL SOC

Published

DOI:10.1021/acssuschemeng.0c02088

Terms of use:

This article is made available under terms and conditions as specified in the corresponding bibliographic description in the repository

Publisher copyright

GENERICO -- per es. Nature : semplice rinvio dal preprint/submitted, o postprint/AAM [ex default]

The original publication is available at <https://pubs.acs.org/doi/10.1021/acssuschemeng.0c02088> / <http://dx.doi.org/10.1021/acssuschemeng.0c02088>.

(Article begins on next page)

1 An Integrated Device for the Solar-Driven Electrochemical 2 Conversion of CO₂ to CO

3 Adriano Sacco,* Roberto Speranza, Umberto Savino, Juqin Zeng, M. Amin Farkhondehfal,
4 Andrea Lamberti,* Angelica Chiodoni, and Candido F. Pirri



Cite This: <https://dx.doi.org/10.1021/acssuschemeng.0c02088>



Read Online

ACCESS |



Metrics & More

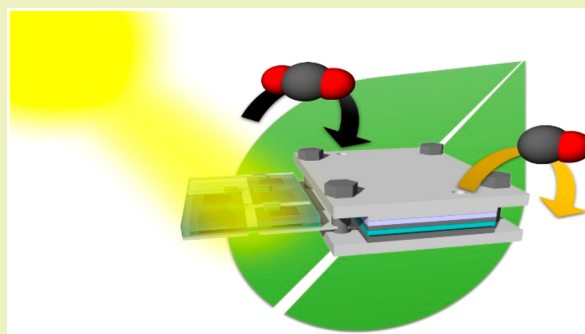


Article Recommendations



Supporting Information

5 **ABSTRACT:** The conversion of carbon dioxide into value-added
6 products using sunlight, also called artificial photosynthesis, represents a
7 remarkable and sustainable approach to store solar energy, transforming
8 it into chemical energy. There are mainly two strategies to carry out this
9 process: the photocatalytic reduction of carbon dioxide (CO₂) or the
10 photovoltaic-powered electrochemical reduction of CO₂. Herein, we
11 focus on the latter route, i.e., the development of a device coupling a
12 solar cell to an electrochemical reactor for CO₂ reduction. Different
13 literature works demonstrated the possibility to achieve such a coupling,
14 but no evidence of a real integration between the two systems has been
15 given up to now. In this work, we present an integrated device
16 constituted by a dye-sensitized solar module (based on a mesoporous
17 titanium dioxide photoanode) and an electrochemical cell (based on a copper–tin
18 cathode). The integration of the two systems is
19 accomplished through a common platinum-based electrode, which acts either as a cathode for the photovoltaic module and as an
20 anode for the electrochemical reactor. The integrated system was characterized by a stable current of 3.6 mA under continuous solar
21 irradiation, enabling the production of 80 mmol of carbon monoxide per day, with a solar-to-fuel efficiency equal to 0.97%.
22 **KEYWORDS:** Artificial photosynthesis, Integrated device, Dye-sensitized solar cells, Photovoltaic module, CO₂ reduction reaction,
23 Electrochemical conversion



23 ■ INTRODUCTION

24 Artificial photosynthesis, i.e., the conversion of solar energy to
25 chemical energy, mimicking the plants' process of natural
26 photosynthesis, has attracted a lot of interest in the scientific
27 community.¹ Essentially, two types of artificial photosynthesis
28 processes are studied by scientists, namely, photocatalytic
29 water splitting,² i.e., the conversion of water into oxygen and
30 hydrogen, and the solar-driven carbon dioxide reduction
31 reaction (CO₂RR), i.e., the conversion of CO₂ to carbon-
32 based value-added products.³ The latter is of particular interest
33 because it would allow attaining a triple goal: (1) storing the
34 excess energy coming from the Sun that is not put in the
35 electric grid,⁴ (2) reduction of atmospheric CO₂, i.e., the major
36 greenhouse gas, which can be used as a raw material,⁵ and (3)
37 production of valuable chemicals.⁶
38 Apart from systems employing photoelectrodes,^{7–9} there are
39 different examples in the literature dealing with solar-driven
40 CO₂ electroreduction obtained by coupling a photovoltaic
41 (PV) device with an electrochemical cell (EC).^{10–17} As an
42 example, Kauffman et al. used a commercial 6 V Si solar
43 module to power a two-chamber electrochemical reactor with a
44 gold (Au) cathode and a platinum (Pt) anode which was able
45 to produce more than 400 L/(g_{Au} h) of carbon monoxide
46 (CO) with a selectivity of about 96%.¹⁰ Schreier and co-

workers employed three series-connected perovskite solar cells 47
to power a single-chamber electrolyzer with a Au cathode¹¹ 48
and studied a triple-junction GaInP/GaInAs/Ge PV device 49
coupled with a dual-chamber EC based on a SnO₂-coated CuO 50
cathode and anode.¹² In both cases, a selectivity toward CO 51
larger than 80% was reached, with solar-to-CO efficiencies 52
equal to 6.5% and 13.4% for perovskite- and triple-junction- 53
based systems, respectively. A 1.4% solar-to-formate efficiency 54
was obtained by White et al. employing a poly-Si solar panel 55
and a three-cell electrolyzer stack composed of indium (In)- 56
based cathodes and iridium oxide (IrO₂)-based anodes.¹³ 57
Moreover, hydrocarbons and oxygenates can be produced by 58
solar-driven CO₂ reduction,¹⁶ with a conversion efficiency 59
larger than 5% by using a III–V/Si tandem PV cell and a two- 60
chamber reactor with a nanostructured copper–silver (Cu– 61
Ag) bimetallic cathode and IrO₂ anode. A lower solar-to- 62
hydrocarbons efficiency equal to 2.3% was obtained by a low- 63

Received: March 16, 2020

Revised: April 16, 2020

Published: May 6, 2020

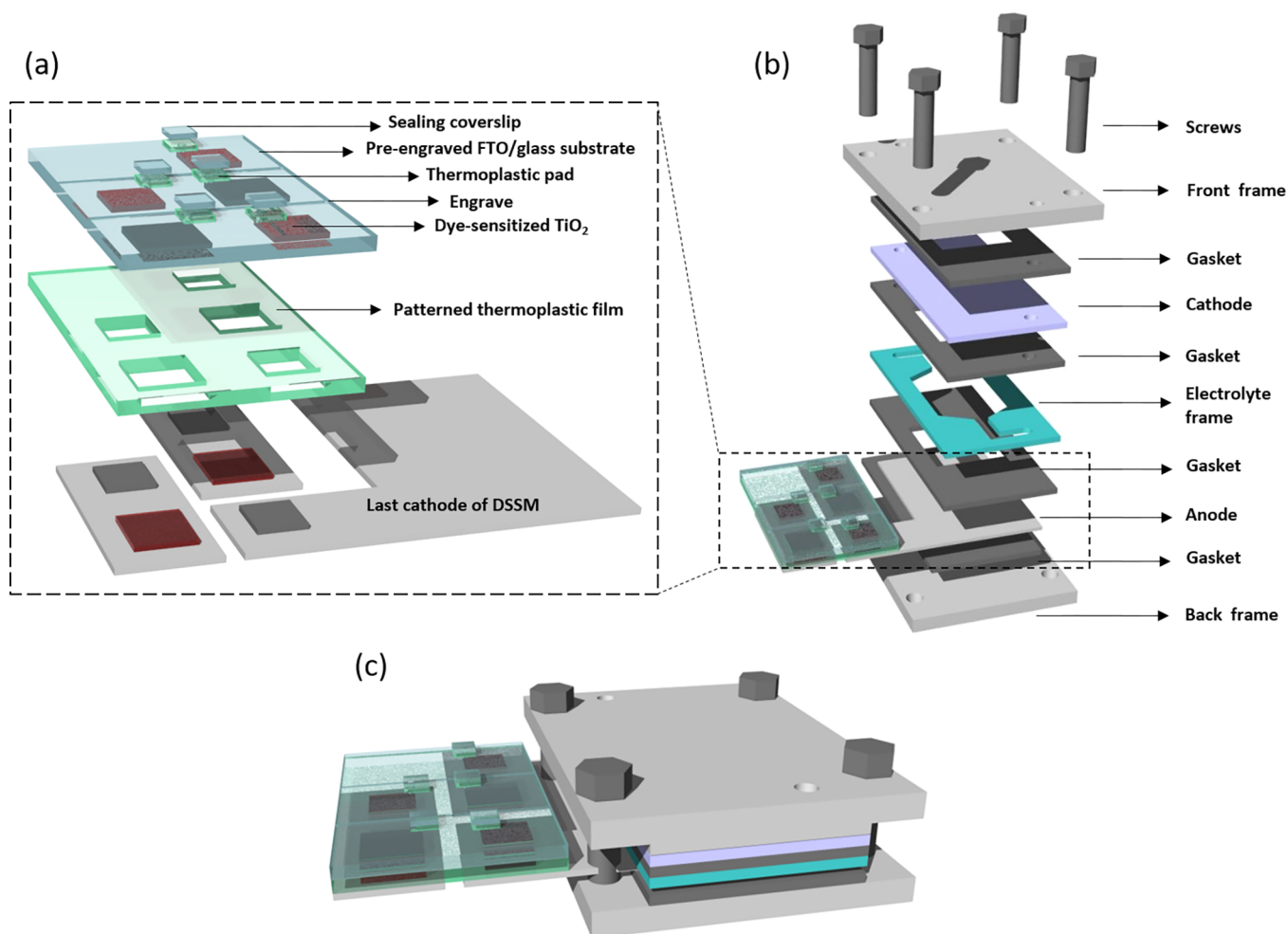


Figure 1. Scheme of the integrated PV–EC system: (a) solar module, (b) electrochemical reactor, and (c) integrated device.

64 cost all-Earth-abundant system, composed of a perovskite PV
 65 minimodule and a two-chamber EC based on nanostructured
 66 CuO for both the cathode and anode.¹⁷ In all of the above-
 67 mentioned and other works,^{14,15,18,19} the PV cell/module is
 68 coupled to the electrochemical reactor through electrical wire
 69 connections, since the solar cell is external or attached to the
 70 electrolyzer. In this sense, we can speak of connected systems,
 71 but no real integrated systems (i.e., with shared electrodes
 72 between the PV and the EC) have been proposed in the
 73 literature so far.

74 In this work, we present, for the first time, an integrated
 75 device for the solar-driven electrochemical conversion of CO₂
 76 to value-added products. To carry out the integration, we
 77 concluded that a third-generation PV technology, namely, dye-
 78 sensitized solar cell (DSSC), makes use of Pt as the cathodic
 79 electrode;²⁰ at the same time, Pt is widely used as the anode
 80 material in EC for CO₂ conversion.^{3,6,10} With these premises,
 81 we fabricated an integrated system in which the Pt electrode is
 82 shared between the dye-sensitized solar module (DSSM) and
 83 the electrochemical reactor, acting at the same time both as
 84 cathode for the solar device and as anode for the EC. The
 85 integrated system was able to carry out the unassisted CO₂
 86 reduction to CO under simulated solar irradiation for more
 87 than 3 h.

RESULTS AND DISCUSSION

88

The PV module is composed of five series-connected DSSCs, 89
 similar to our previous work,²¹ with an increase in the cell 90
 number to five in order to achieve an operating voltage higher 91
 than 2.5 V. The module employed a nanocrystalline TiO₂ 92
 photoanode, Ru-based sensitizer, iodide/tri-iodide electrolyte, 93
 and Pt cathode. Two different current collectors were selected 94
 for module fabrication: transparent conductive substrate as the 95
 front side (top of the device) and titanium foils as the back 96
 side (bottom of the device). Details of the fabrication 97
 procedure are reported in the [Supporting Information](#). The 98
 dimension of the last cathode of the cell series was chosen in 99
 order to overpass the PV module footprint and act as the 100
 anode for the EC. Concerning the EC, a single-chamber 101
 configuration was employed, in which no membrane was used 102
 to separate the anode and the cathode, as shown in [Figure 1](#). 103 f1
 This configuration has been adopted in order to reduce the 104
 total cell overpotential by eliminating the proton exchange 105
 membrane (see [Supporting Information](#) for details).^{11,22} A 106
 Cu–Sn electrocatalyst recently proposed by our group,^{23,24} 107
 characterized by a good selectivity toward CO, was used as the 108
 cathodic material. The Cu–Sn cathode was prepared through a 109
 cost-efficient electrodeposition route, as detailed in the 110
[Supporting Information](#). The already mentioned Ti-supported 111
 Pt was employed as the anode. A CO₂-saturated 0.1 M 112
 KHCO₃ aqueous solution was chosen as the electrolyte. The 113

114 volume of the electrolyte was 7 mL, with a 3 mL headspace. A
 115 scheme of the integrated device is depicted in Figure 1.
 116 The performance of the two components of the system was
 117 first investigated individually. Figure 2 shows the current–

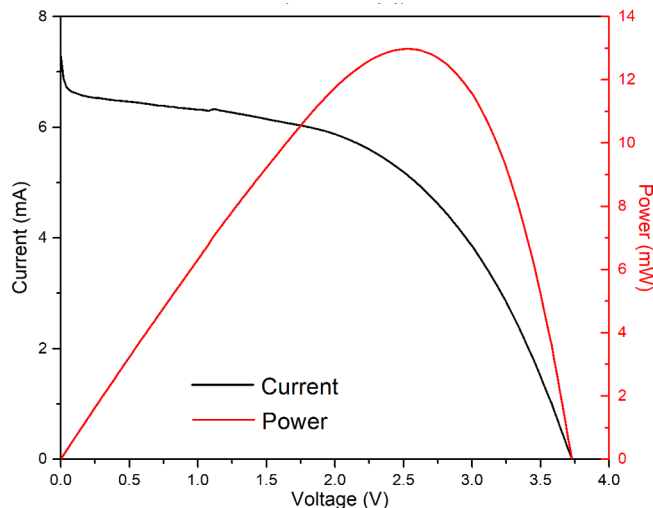


Figure 2. Current–voltage characteristic of the five-cell PV module under 1 sun illumination (left axis) and corresponding produced power (right axis).

118 voltage characteristic of the PV model acquired under AM1.5G
 119 illumination. By comparing the curve in Figure 2 with the data
 120 reported for our previously published DSSM,²¹ it can be
 121 observed that the addition of the fifth solar cell in the PV
 122 module leads to a boost of the voltage with respect to the four-
 123 cell module, with an open circuit value of 3.73 V, i.e., almost a
 124 1 V increase. This improvement cannot be simply justified with
 125 the addition of a cell since it is larger than the open circuit
 126 voltage (V_{oc}) of a traditional DSSC (based on the combination
 127 of TiO_2 , Ru-based dye and I^-/I_3^-). Therefore, it must be
 128 ascribed to the different architectures of the two DSSM.
 129 Indeed, in the present study, Ti foils are used as current
 130 collectors on one side of the module to allow integration with
 131 the electrochemical reactor for CO_2 reduction, while fluorine-
 132 doped tin oxide (FTO)-coated glasses were used by Scalia et
 133 al.²¹ This variation induces two main effects: (i) the reduction
 134 of the series resistance (accounting for the transport resistance
 135 of the substrate) due to a higher conductivity of Ti with
 136 respect to FTO and (ii) the *in situ* formation of a TiO_2
 137 blocking layer on the Ti surface during the thermal treatment
 138 for photoanode preparation. While the former can influence
 139 the photogenerated current, the latter can be considered as the
 140 main reason responsible for the increased V_{oc} of the present
 141 DSSM. In fact, it is well known that the introduction of a very
 142 thin TiO_2 layer between the current collector and the
 143 nanostructured photoanode film allows for preventing electron
 144 recombination with a positive effect on the V_{oc} .²⁵ For what
 145 concerns the other parameters, both the PV modules exhibit
 146 similar currents (short circuit value of about 7 mA) and fill
 147 factors (0.48), thus leading to an enhanced photoconversion
 148 efficiency of 2.68% for the novel five-cell device. It is worth
 149 noting that a maximum power of 13 mW is produced by the
 150 DSSM at 2.54 V and that power larger than 10 mW can be
 151 obtained in the wide voltage range of 1.7–3.2 V.
 152 The performance of the EC was assessed through 1 h CO_2
 153 electrolysis tests at different voltages. A micro-gas chromato-

graph (μGC) was used for the online measurements of the
 gaseous products, and a high-performance liquid chromatog-
 raph (HPLC) was used for the analysis of the liquid products
 at the end of each test.²⁶ During the experiments, a constant
 CO_2 flow of 10 mL/min was maintained in order to saturate
 the electrolyte and to carry the gaseous products to the μGC .
 Figure 3 reports the faradaic efficiency (FE) for the different

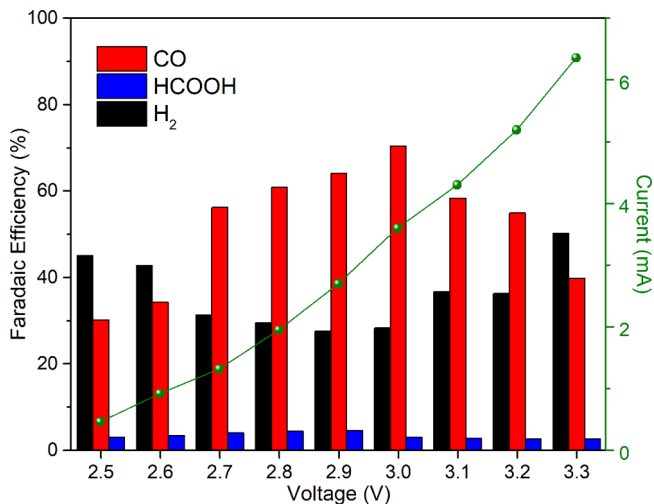


Figure 3. Faradaic efficiencies for CO , $HCOOH$, and H_2 formation in EC at various applied voltages during 1 h electrolysis (left axis) and corresponding measured currents (right axis).

reaction products as a function of the applied voltage. Only
 CO and H_2 were detected as gaseous products, while just
 formic acid ($HCOOH$) was identified as the liquid product.
 With the exception of low (≤ 2.6 V) and high (≥ 3.3 V)
 voltages, the CO_2RR outperforms the competing hydrogen
 evolution reaction, thus confirming the goodness of our Cu-
 based electrocatalyst.^{23,24} A maximum FE for CO production
 of about 73% was obtained at 3.0 V, where the total measured
 current is 3.6 mA (corresponding to a cathodic current density
 of 6.4 mA/cm^2). By comparing this data with those of the PV
 module, an optimal operating point at 3.0 V can be envisaged
 for the integrated system since the solar device produces a
 similar current of 3.7 mA at this voltage.

Figure 4a shows the measured current–voltage characteristic
 of the PV module under 1 sun illumination superimposed to
 that of the EC. As anticipated above, the theoretical operating
 point, given by the intersection of the two curves, can be found
 at 3.0 V. At this potential, the power produced by the PV
 module is 11.5 mW, and the partial current (density) for CO
 production is equal to 2.6 mA (4.7 mA/cm^2). The electrolysis
 experiment on the integrated PV–EC system was carried out
 under 1 sun illumination for more than 3 h, during which the
 produced gases were measured by μGC (the liquid products
 were measured after the test through HPLC). The results of
 this measurement are reported in Figure 4b and c. The
 integrated device is characterized by a constant voltage of 3.00 ± 0.06 V
 for all the period of investigation and a by corresponding stable
 current density equal to $6.5 \pm 0.4 \text{ mA/cm}^2$ after 30 min of operation
 (Figure 4b). It is worth noting that such a stability is in line
 with or even better than those reported for nonintegrated PV–EC
 systems.^{7,14,18} In the initial phase of the electrolysis, the
 decrease in the current density is associated with the reduction
 of oxide species in the Cu–Sn

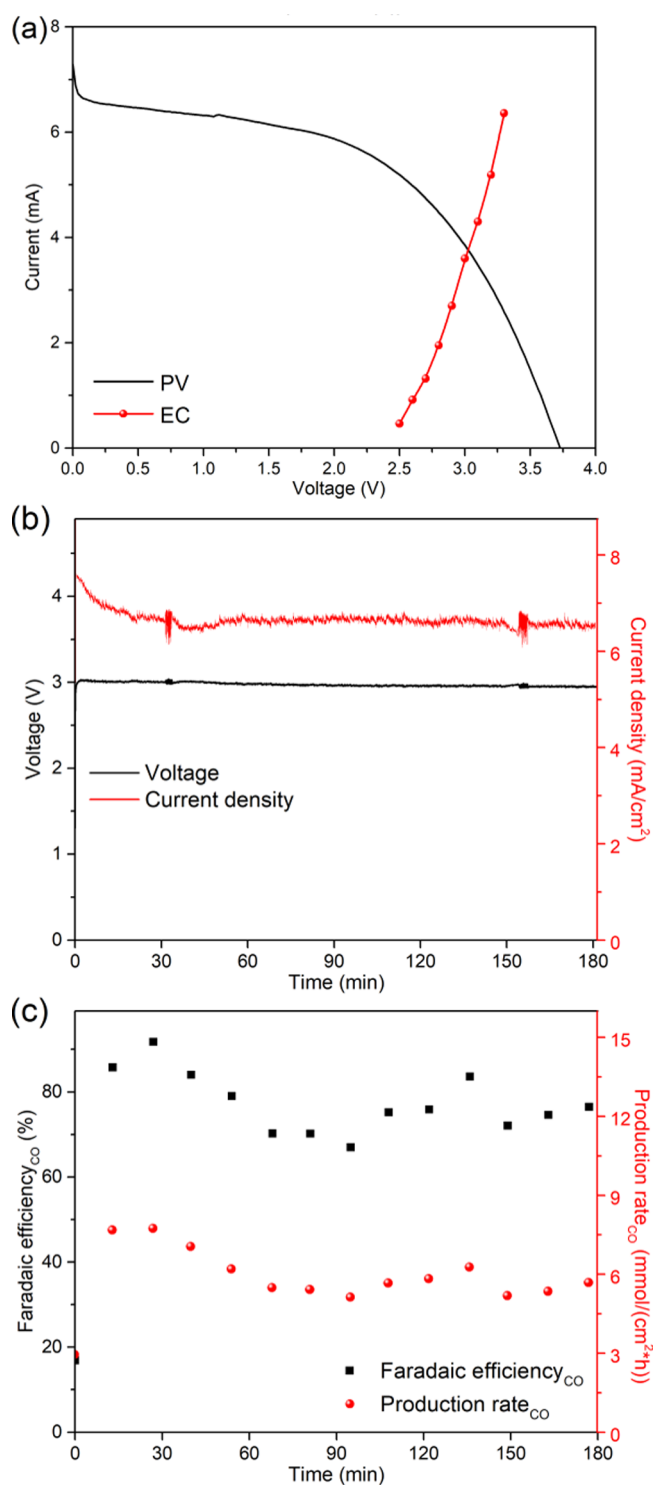


Figure 4. (a) Current–voltage characteristic of the five-cell PV module under 1 sun illumination and of the EC. (b) Voltage (left axis) and current density (right axis) during a 3 h test of the integrated PV–EC system under 1 sun illumination. (c) FE (left axis) and production rate (right axis) for CO during a 3 h test of the integrated PV–EC system under 1 sun illumination.

stable during 3 h of operation, thus proving that sunlight and CO₂ can be efficiently and continuously converted by our integrated device, similarly to PV–EC coupled systems present in the literature.^{11,12,17} A CO production rate of about 80 mmol/day (considering 24 h of continuous operation) was obtained along the 3 h test.

The obtained data was employed to calculate the solar-to-CO efficiency η_{STC} of our integrated system, according to the formula

$$\eta_{\text{STC}} = \frac{E_{\text{CO}_2/\text{CO}}^0 \cdot J \cdot \text{FE}_{\text{CO}}}{W_{\text{sol}}} \quad (1)$$

where $E_{\text{CO}_2/\text{CO}}^0$ is the standard cell potential when the EC conducts the CO₂RR to CO (equal to 1.34 V), J is the current density of the PV module, FE_{CO} is the faradaic efficiency for CO, and W_{sol} is the solar irradiance.¹¹ A solar-to-CO efficiency equal to 0.79% is found for our integrated PV–EC system. This efficiency can be further increased considering also H₂ as a secondary product (for example, for the production of syngas),²⁷ leading to a total solar-to-fuel efficiency of 0.97%. The obtained values are comparable to the efficiencies presented in the literature for coupled PV–EC systems.¹⁴ Better results have been also reported.^{11,17,18} However, it has to be highlighted that the performance of our integrated PV–EC system can be improved since different aspects can be optimized:

- An additional PV cell can be added to the module in order to enlarge the voltage window of the module and shift the operating point in a region of higher cell efficiency.
- Adapting the active area of the PV module to the electrocatalyst one can be done in order to match the two currents.

These aspects have already been taken into consideration in a new work which is in progress in our lab. Nevertheless, the present work demonstrates the feasibility of an integrated PV–EC system that enables the solar-driven electrochemical conversion of CO₂.

CONCLUSION

An integrated system composed of a third-generation PV module and an EC for the electroreduction of CO₂ under solar illumination has been presented here. The PV module is based on a series of five DSSCs, while the EC is based on a Cu–Sn electrocatalyst. The integration of the two devices has been achieved through a common Pt-based electrode, which works both as a cathode for the PV module and as an anode for the EC.

A stable voltage of 3 V has been obtained from the integrated system under 1 sun illumination for 3 h, during which CO production with a FE of 78% was achieved as a result of the unassisted CO₂RR. This represents the first integrated artificial photosynthesis device for the solar-driven electrochemical conversion of CO₂. This system is currently under optimization in our laboratory in order to improve the overall device efficiency.

ASSOCIATED CONTENT

Supporting Information

The Supporting Information is available free of charge at <https://pubs.acs.org/doi/10.1021/acssuschemeng.0c02088>.

cathode.^{23,24} In accordance with the analysis conducted on the bare EC, only CO and HCOOH were detected as CO₂RR products, with average FE values equal to about 78% and 2%, respectively. The FE for CO is plotted as a function of the electrolysis time in Figure 4c. It can be observed that it remains

256 Experimental section, measurements of membrane
257 overpotential, scheme of DSSM, scheme of EC, and
258 pictures of the integrated PV–EC device (PDF)

259 ■ AUTHOR INFORMATION

260 Corresponding Authors

261 **Adriano Sacco** – Center for Sustainable Future Technologies @
262 Polito, Istituto Italiano di Tecnologia, 10144 Torino, Italy;

263 orcid.org/0000-0002-9229-2113; Phone: +39 011

264 5091912; Email: adriano.sacco@iit.it; Fax: +39 011

265 5091901

266 **Andrea Lamberti** – Center for Sustainable Future Technologies
267 @Polito, Istituto Italiano di Tecnologia, 10144 Torino, Italy;

268 Applied Science and Technology Department, Politecnico di
269 Torino, Corso Duca degli Abruzzi, 10129 Torino, Italy;

270 orcid.org/0000-0003-4100-9661; Phone: +39 011

271 0907394; Email: andrea.lamberti@polito.it; Fax: +39 011

272 0907399

273 Authors

274 **Roberto Speranza** – Center for Sustainable Future Technologies
275 @Polito, Istituto Italiano di Tecnologia, 10144 Torino, Italy;

276 Applied Science and Technology Department, Politecnico di
277 Torino, Corso Duca degli Abruzzi, 10129 Torino, Italy

278 **Umberto Savino** – Center for Sustainable Future Technologies
279 @Polito, Istituto Italiano di Tecnologia, 10144 Torino, Italy;

280 Applied Science and Technology Department, Politecnico di
281 Torino, Corso Duca degli Abruzzi, 10129 Torino, Italy

282 **Juqin Zeng** – Center for Sustainable Future Technologies @
283 Polito, Istituto Italiano di Tecnologia, 10144 Torino, Italy

284 **M. Amin Farkhondehfal** – Center for Sustainable Future
285 Technologies @Polito, Istituto Italiano di Tecnologia, 10144

286 Torino, Italy

287 **Angelica Chiodoni** – Center for Sustainable Future
288 Technologies @Polito, Istituto Italiano di Tecnologia, 10144

289 Torino, Italy

290 **Candido F. Pirri** – Center for Sustainable Future Technologies
291 @Polito, Istituto Italiano di Tecnologia, 10144 Torino, Italy;

292 Applied Science and Technology Department, Politecnico di
293 Torino, Corso Duca degli Abruzzi, 10129 Torino, Italy

294 Complete contact information is available at:

295 <https://pubs.acs.org/10.1021/acssuschemeng.0c02088>

296 Author Contributions

297 The manuscript was written through contributions of all
298 authors. All authors have given approval to the final version of
299 the manuscript.

300 Notes

301 The authors declare no competing financial interest.

302 ■ REFERENCES

303 (1) Saracco, G.; Vankova, S.; Pagliano, C.; Bonelli, B.; Garrone, E.
304 Outer Co(II) Ions in Co-ZIF-67 Reversibly Adsorb Oxygen from
305 Both Gas Phase and Liquid Water. *Phys. Chem. Chem. Phys.* **2014**, *16*,
306 6139–6145.

307 (2) Hernández, S.; Tortello, M.; Sacco, A.; Quaglio, M.; Meyer, T.;
308 Bianco, S.; Saracco, G.; Pirri, C. F.; Tresso, E. New Transparent
309 Laser-Drilled Fluorine-Doped Tin Oxide Covered Quartz Electrodes
310 for Photo-Electrochemical Water Splitting. *Electrochim. Acta* **2014**,
311 *131*, 184–194.

312 (3) Sacco, A. Electrochemical Impedance Spectroscopy as a Tool to
313 Investigate the Electroreduction of Carbon Dioxide: A Short Review.
314 *J. CO₂ Util.* **2018**, *27*, 22–31.

(4) Bushuyev, O. S.; De Luna, P.; Dinh, C. T.; Tao, L.; Saur, G.; van
de Lagemaat, J.; Kelley, S. O.; Sargent, E. H. What Should We Make
with CO₂ and How Can We Make It? *Joule* **2018**, *2*, 825–832.

(5) Sacco, A.; Zeng, J.; Bejtka, K.; Chiodoni, A. Modeling of Gas
Bubble-Induced Mass Transport in the Electrochemical Reduction of
Carbon Dioxide on Nanostructured Electrodes. *J. Catal.* **2019**, *372*,
39–48.

(6) Farkhondehfal, M. A.; Hernández, S.; Rattalino, M.; Makkee, M.;
Lamberti, A.; Chiodoni, A.; Bejtka, K.; Sacco, A.; Pirri, C. F.; Russo,
N. Syngas Production by Electrocatalytic Reduction of CO₂ Using
Ag-Decorated TiO₂ Nanotubes. *Int. J. Hydrogen Energy* **2019**, *na*, na
DOI: 10.1016/j.ijhydene.2019.04.180.

(7) Zhou, X.; Liu, R.; Sun, K.; Chen, Y.; Verlage, E.; Francis, S. A.;
Lewis, N. S.; Xiang, C. Solar-Driven Reduction of 1 Atm of CO₂ to
Formate at 10% Energy-Conversion Efficiency by Use of a TiO₂-
Protected III-V Tandem Photoanode in Conjunction with a Bipolar
Membrane and a Pd/C Cathode. *ACS Energy Lett.* **2016**, *1*, 764–770.

(8) Liang, L.; Lei, F.; Gao, S.; Sun, Y.; Jiao, X.; Wu, J.; Qamar, S.;
Xie, Y. Single Unit Cell Bismuth Tungstate Layers Realizing Robust
Solar CO₂ Reduction to Methanol. *Angew. Chem., Int. Ed.* **2015**, *54*,
13971–13974.

(9) Asadi, M.; Kim, K.; Liu, C.; Addepalli, A. V.; Abbasi, P.; Yasaei,
P.; Phillips, P.; Behranginia, A.; Cerrato, J. M.; Haasch, R.; Zapol, P.;
Kumar, B.; Klie, R. F.; Abiade, J.; Curtiss, L. A.; Salehi-Khojin, A.
Nanostructured Transition Metal Dichalcogenide Electrocatalysts for
CO₂ Reduction in Ionic Liquid. *Science* **2016**, *353*, 467–470.

(10) Kauffman, D. R.; Thakkar, J.; Siva, R.; Matranga, C.;
Ohodnicki, P. R.; Zeng, C.; Jin, R. Efficient Electrochemical CO₂
Conversion Powered by Renewable Energy. *ACS Appl. Mater.*
Interfaces **2015**, *7*, 15626–15632.

(11) Schreier, M.; Curvat, L.; Giordano, F.; Steier, L.; Abate, A.;
Zakeeruddin, S. M.; Luo, J.; Mayer, M. T.; Grätzel, M. Efficient
Photosynthesis of Carbon Monoxide from CO₂ Using Perovskite
Photovoltaics. *Nat. Commun.* **2015**, *6*, 7326.

(12) Schreier, M.; Héroguel, F.; Steier, L.; Ahmad, S.; Luterbacher, J.
S.; Mayer, M. T.; Luo, J.; Grätzel, M. Solar Conversion of CO₂ to CO
Using Earth-Abundant Electrocatalysts Prepared by Atomic Layer
Modification of CuO. *Nat. Energy* **2017**, *2*, 17087.

(13) White, J. L.; Herb, J. T.; Kaczur, J. J.; Majsztrik, P. W.; Bocarsly,
A. B. Photons to Formate: Efficient Electrochemical Solar Energy
Conversion Via Reduction of Carbon Dioxide. *J. CO₂ Util.* **2014**, *7*,
1–5.

(14) Ren, D.; Loo, N. W. X.; Gong, L.; Yeo, B. S. Continuous
Production of Ethylene from Carbon Dioxide and Water Using
Intermittent Sunlight. *ACS Sustainable Chem. Eng.* **2017**, *5*, 9191–
9199.

(15) Sriramagiri, G. M.; Ahmed, N.; Luc, W.; Dobson, K. D.;
Hegedus, S. S.; Jiao, F. Toward a Practical Solar-Driven CO₂ Flow
Cell Electrolyzer: Design and Optimization. *ACS Sustainable Chem.*
Eng. **2017**, *5*, 10959–10966.

(16) Gurudayal; Bullock, J.; Srankó, D. F.; Towle, C. M.; Lum, Y.;
Hettick, M.; Scott, M. C.; Javey, A.; Ager, J. Efficient Solar-Driven
Electrochemical CO₂ Reduction to Hydrocarbons and Oxygenates.
Energy Environ. Sci. **2017**, *10*, 2222–2230.

(17) Huan, T. N.; Dalla Corte, D. A.; Lamaison, S.; Karapinar, D.;
Lutz, L.; Menguy, N.; Foldyna, M.; Turren-Cruz, S.-H.; Hagfeldt, A.;
Bella, F.; Fontecave, M.; Mougél, V. Low-Cost High-Efficiency
System for Solar-Driven Conversion of CO₂ to Hydrocarbons. *Proc.*
Natl. Acad. Sci. U. S. A. **2019**, *116*, 9735–9740.

(18) Urbain, F.; Tang, P.; Carretero, N. M.; Andreu, T.; Gerling, L.
G.; Voz, C.; Arbiol, J.; Morante, J. R. A Prototype Reactor for Highly
Selective Solar-Driven CO₂ Reduction to Synthesis Gas Using
Nanosized Earth-Abundant Catalysts and Silicon Photovoltaics.
Energy Environ. Sci. **2017**, *10*, 2256–2266.

(19) Sugano, Y.; Ono, A.; Kitagawa, R.; Tamura, J.; Yamagiwa, M.;
Kudo, Y.; Tsutsumi, E.; Mikoshiba, S. Crucial Role of Sustainable
Liquid Junction Potential for Solar-to-Carbon Monoxide Conversion
by a Photovoltaic Photoelectrochemical System. *RSC Adv.* **2015**, *5*,
54246–54252.

- 384 (20) Sacco, A. Electrochemical Impedance Spectroscopy: Funda-
385 mentals and Application in Dye-Sensitized Solar Cells. *Renewable*
386 *Sustainable Energy Rev.* **2017**, *79*, 814–829.
- 387 (21) Scalia, A.; Varzi, A.; Lamberti, A.; Tresso, E.; Jeong, S.; Jacob,
388 T.; Passerini, S. High Energy and High Voltage Integrated Photo-
389 Electrochemical Double Layer Capacitor. *Sustain. Energy Fuels* **2018**,
390 *2*, 968–977.
- 391 (22) Singh, M. R.; Clark, E. L.; Bell, A. T. Effects of Electrolyte,
392 Catalyst, and Membrane Composition and Operating Conditions on
393 the Performance of Solar-Driven Electrochemical Reduction of
394 Carbon Dioxide. *Phys. Chem. Chem. Phys.* **2015**, *17*, 18924–18936.
- 395 (23) Zeng, J.; Bejtka, K.; Ju, W.; Castellino, M.; Chiodoni, A.; Sacco,
396 A.; Farkhondehfar, M. A.; Hernández, S.; Rentsch, D.; Battaglia, C.;
397 Pirri, C. F. Advanced Cu-Sn Foam for Selectively Converting CO₂ to
398 CO in Aqueous Solution. *Appl. Catal., B* **2018**, *236*, 475–482.
- 399 (24) Ju, W.; Zeng, J.; Bejtka, K.; Ma, H.; Rentsch, D.; Castellino, M.;
400 Sacco, A.; Pirri, C. F.; Battaglia, C. Sn-Decorated Cu for Selective
401 Electrochemical CO₂ to CO Conversion: Precision Architecture
402 Beyond Composition Design. *ACS Appl. Energy Mater.* **2019**, *2*, 867–
403 872.
- 404 (25) Bella, F.; Sacco, A.; Pugliese, D.; Laurenti, M.; Bianco, S.
405 Additives and Salts for Dye-Sensitized Solar Cells Electrolytes: What
406 Is the Best Choice? *J. Power Sources* **2014**, *264*, 333–343.
- 407 (26) Bejtka, K.; Zeng, J.; Sacco, A.; Castellino, M.; Hernández, S.;
408 Farkhondehfar, M. A.; Savino, U.; Ansaloni, S.; Pirri, C. F.; Chiodoni,
409 A. Chainlike Mesoporous SnO₂ as a Well-Performing Catalyst for
410 Electrochemical CO₂ Reduction. *ACS Appl. Energy Mater.* **2019**, *2*,
411 3081–3091.
- 412 (27) Zeng, J.; Bejtka, K.; Di Martino, G.; Sacco, A.; Castellino, M.;
413 Re Fiorentin, M.; Risplendi, F.; Farkhondehfar, M. A.; Hernández, S.;
414 Cicero, G.; Pirri, C. F.; Chiodoni, A. Microwave-Assisted Synthesis of
415 Copper-Based Electrocatalysts for Converting Carbon Dioxide to
416 Tunable Syngas. *ChemElectroChem* **2020**, *7*, 229–238.